Mon. Not. R. Astron. Soc. **389,** 205–212 (2008) doi:10.1111/j.1365-2966.2008.13528.x

Spectroscopic and photometric analysis of NSV 24512: an early-type eclipsing binary embedded in a dust cloud⋆

Ö. Çakırlı,[1]† C. İbanoğlu,[1] J. Southworth,[2] A. Frasca[3] and J. Hernandez[4]

[1]*Ege University, Science Faculty, Astronomy and Space Sciences Department, 35100 Bornova, İzmir, Turkey*
[2]*Department of Physics, University of Warwick, Coventry, CV4 7AL*
[3]*INAF – Catania Astrophysical Observatory, via S. Sofia 78, I-95123, Catania, Italy*
[4]*Department of Astronomy, University of Michigan, Ann Harbor, MI 48109-1090, USA*

Accepted 2008 May 30. Received 2008 May 23; in original form 2008 February 29

ABSTRACT

We present differential *V*-band photometric observations and the first radial velocities of NSV 24512, which is embedded in the Serpens star-forming region. This double-lined system has an eccentric orbit with an eccentricity of 0.193. The system is a member of visual double star ADS 11410AB with a separation of about 0.3 arcsec and an apparent visual magnitude difference of 0.125 mag; we find that the fainter component (component B) is responsible for the periodic light variation. Therefore, we subtracted the light contribution of component A from the total light. The *V*-band photometric data and radial velocities were then analysed simultaneously using the Wilson–Devinney program. From the blue-wavelength spectroscopic observations and radial velocities, we classify the primary and secondary components as B8V and B9V stars, respectively. The masses and radii of the component stars have been derived as 3.68 ± 0.05 and $3.36 \pm 0.04\,M_{\odot}$ and 3.21 ± 0.05 and $2.93 \pm 0.05\,R_{\odot}$, respectively. Comparison with theoretical evolutionary models indicates that both components are pre-main-sequence stars with an age of about 2.1 Myr. The projected rotational velocities of the components measured by us are much smaller than the synchronous rotational velocities. The high asynchronism is further evidence of the very young age of the system. Using the radiative properties of the stars, we have redetermined the distance to NSV 24512 as 247 ± 5 pc, which is in good agreement with, and more precise than, previous determinations. Adopting the same interstellar extinction and distance, we classify component A to be of spectral type B7, if it is a single star.

Key words: binaries: close – binaries: eclipsing – binaries: general – binaries: spectroscopic – stars: individual: NSV 24512.

1 INTRODUCTION

The light variability of NSV 24512 (BD −00° 3513, HD 171491, HIP 91113, $V \simeq 8\overset{\mathrm{m}}{.}0$) was discovered by the *Hipparcos* satellite (Perryman et al. 1997). It was classified as a detached Algol-type eclipsing binary by Otero (2005), with the primary and secondary eclipses having almost equal depths of about 0.14 mag. Before its discovery as a variable star, Rufener & Bartholdi (1982) listed the star in the variable, microvariable or suspected variable stars detected in the Geneva photometric system. Chavarria et al. (1988) indicated that NSV 24512 belongs to the Serpens dark cloud, which is known to contain an extremely young star cluster. As a reflection nebula, it displays some signs of recent or ongoing star formation. In addition, it has molecular clouds of CO, H_2CO and NH_3, masers, near- and far-infrared sources, Herbig–Haro-like objects, pre-main-sequence stars with Hα in emission, and intermediate-temperature stars with associated reflection nebulosity (e.g. Chavarria et al. 1988). Nearly two decades ago, an examination of the *IRAS* all-sky images presented a new opportunity to reveal some clues about the interactions of hot stars with their surrounding materials (Van Buren & McCray 1988). The presence of a U-shaped stellar wind bow shock around NSV 24512 has been shown by Van Buren, Noriega-Crespo & Dgani (1995).

As the system is located in an ongoing star formation region, it has been the subject of various investigations. The first spectral classification of the star was made by Rufener & Bartholdi (1982) as B5, using the Geneva photometric system. Later, Chavarria et al. (1988) obtained *uvby–JHKLM* photometry and median-resolution spectra of VV Serpentis and of 12 stars in the reflection nebulae.

⋆Based on observations collected at Catania Astrophysical Observatory (Italy) and Ege University Observatory (Turkey).

†E-mail: omur.cakirli@gmail.com

They estimated the spectral type and luminosity class of NSV 24512 as B3 V and B3.5 V from spectroscopic and photometric data, respectively. Subsequent *uvbyβ* observations performed by Knude (1992) revealed that NSV 24512 appears in the most heavily reddened six stars in both the $m_1-(b-y)$ and $c_1-(b-y)$ diagrams among the 528 B-type stars of interest. The near-infrared *JHKL* observations of reflection nebulosity stars associated with the Serpens dark cloud region, obtained by Lara, Chavarria & Lopez-Molina (1991), were combined with the earlier *uvbyβ* photometric data to measure the distance to the Serpens cloud and the mean visual extinction ratio. They estimated a reddening in the *B–V* colour excess of about 1.2 mag, with large reddening variations within the cloud. Straizys, Cernis & Bartasiute (1996) observed 105 stars in the Serpens molecular cloud area with the Vilnius seven-colour photometric system. They concluded that the star NSV 24512 is among the most heavily reddened five stars with $E(B-V) = 0.75$ mag and $A_v = 2.46$ mag.

However, *Hipparcos* (Perryman et al. 1997) discovered 187 multiple systems (Double and Multiple Annex: Part C), one of which is NSV 24512 (ADS 11410, CCDM 18351+0003). However, the SIMBAD data base lists the star ADS 11410 as a triple system with a third component of about 12 mag. The apparent visual magnitudes of the components A and B were measured by the *Hipparcos* satellite as 8.768 and 8.893 mag, separated by 0.275 arcsec. Although the star NSV 24512 is not seen in the current version of the Multiple Star Catalogue (Tokovinin 1997), which contains 905 physical multiple (i.e. double, triple, quadruple, etc.) star systems, the last version of the Washington Double Star Catalogue (Hartkopf, Mason & McAlister 2005) includes it with a separation of 0.2 arcsec and apparent visual magnitudes of 8.77 and 8.89 mag. A total magnitude of 7.8 mag and a composite spectral type of B5 was assigned.

Multiple star systems are frequently found in star-forming regions such as dark molecular clouds. The reasons for studying the spectroscopic and photometric properties of multiple stars are numerous. Their physical parameters and location may have a major impact on the evolution of their parental molecular clouds. Reliable spectral types of young stellar objects, such as NSV 24512, are important not only in determining their physical characteristics but also for yielding valuable information about the physical environment surrounding these young stars. The value of total-to-selective extinction and infrared excesses yields some signs about the chemical composition of the parental cloud.

The primary aim of the present paper is to present new spectroscopic and photometric observations of the detached eclipsing binary NSV 24512, to obtain the first almost complete light and radial velocity (RV) curves, and to determine the physical characteristics of the components by analysing the available data simultaneously. The observations and data reduction are described in Section 2. The times of minima are listed and the new orbital period is determined in Section 3, and the simultaneous analyses of the RVs and *V*-band light curve are presented in Section 4. Finally, the results are discussed and summarized in Section 5.

2 OBSERVATIONS

2.1 *V*-band light curve

NSV 24512 was observed by *Hipparcos* between 1989 and 1993. Otero (2005) combined the *Hipparcos* data with those obtained by ASAS-3 (Pojmanski 2002) to reveal the first *V*-band light curve of this system. It has been classified as an Algol-type binary with an orbital period of $2^{\rm d}.2597$ from visual inspection of the light variation.

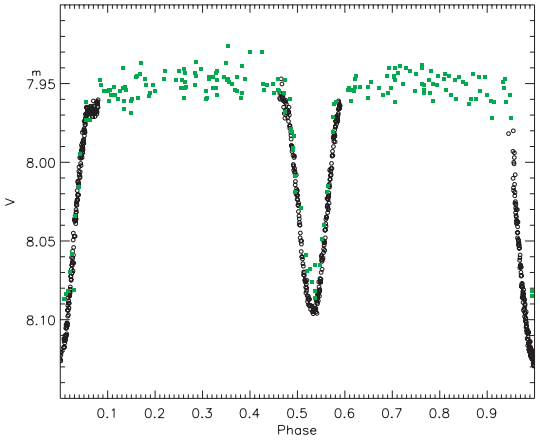

Figure 1. The observed *V*-band light curve for NSV 24512. The filled squares and open circles correspond to the data obtained by ASAS-3 and by us, respectively.

The depths of the primary and secondary eclipses are nearly the same in this first light curve.

We observed NSV 24512 photometrically with the 40-cm telescope of the Ege University Observatory between 2007 April and August, using Bessel *BVR* filters. The telescope was equipped with a CCD camera hosting a 2k × 2k CCD cooled to −25°C. The field of view of the detector was 12.8 × 12.8 arcmin^2 and the scale was 0.32 arcsec per pixel. Dark frames and flat fields were also obtained, and standard image processing was carried out. The reduction was carried out using the IRAF[1] DAOPHOT package (Massey & Davis 1992). Because the field of NSV 24512 is not crowded, the technique of aperture photometry was applied to extract the differential magnitudes. The individual measurements were obtained differentially with respect to BD −00° 3514. BD −00° 3515 was chosen as a check star. We observed the system particularly during the eclipses for two reasons: to reveal which of the eclipses corresponds to the primary minimum and to make a preliminary estimate of the apsidal motion rate. We have combined the *V*-band photometric data of NSV 24512 obtained between 2001 and 2005 with those obtained by us (Fig. 1). The depths of the primary and secondary eclipses are about 0.177 and 0.144 mag, respectively. Moreover, the secondary eclipse appears at phase 0.534, showing that the orbit is eccentric.

2.2 Spectroscopic observations

Spectroscopic observations were performed with the echelle spectrograph (FRESCO) at the 91-cm telescope of the Catania Astrophysical Observatory (OAC). Spectra were recorded on a CCD camera equipped with a thinned back-illuminated SITe (Scientific Imaging Technologies) CCD of 1k × 1k pixel (size 24 × 24 μm^2). The echelle crossed-dispersed configuration yields a resolution of about 21 000, as deduced from the full width at half-maximum (FWHM) of the lines of the Th–Ar calibration lamp. The spectra cover the wavelength range from 4300 to 6650 Å, split into 19 orders. In this spectral region, and in particular in the blue portion of the spectrum, there are several lines useful for the measurement of

[1] IRAF is distributed by the National Optical Astronomy Observatories, which are operated by the Association of Universities for Research in Astronomy, Inc., under contract to the National Science Foundation.

RVs (Andersen 1975), as well as for the spectral classification of the stars.

The data reduction was performed using the echelle task of the IRAF package following the standard steps: background subtraction, division by a flat-field spectrum given by a halogen lamp, wavelength calibration using the emission lines of a Th–Ar lamp, and normalization to the continuum through a polynomial fit.

In order to confirm the eclipsing binary nature of the system, and to derive the orbital parameters, 21 spectra of NSV 24512 were collected during the 22 observing nights between 2006 August 2 and 23. The exposure times were typically between 2400 and 3000 s. The signal-to-noise ratio (S/N) achieved was between 54 and 121, depending on atmospheric conditions.

In addition to NSV 24512, we also observed some reference stars, whose spectral types are similar to the components of our target system. We have chosen non-active and slowly rotating standard stars. Bright stars with low $v \sin i$, α Lyr (A0 V, $V_r = 24$ km s^{-1}), HD 27962 (A2 IV, $V_r = 15$ km s^{-1}) and τ Her (B5 IV, $V_r = -12.7$ km s^{-1}), were chosen as templates for the RV measurements of the hotter and cooler components, and were observed on each night during our observational run. We used τ Her as a template because its spectral type is very close to our target NSV 24512 and it has moderate $v \sin i$, which gives the smallest RV errors.

In the present work, the RVs of the components of NSV 24512 were derived by means of cross-correlation functions (CCFs) using the IRAF task FXCOR (e.g. Tonry & Davis 1979; Popper & Jeong 1994). Near the quadrature phases, the He I 5876 Å line of the primary and secondary components of the close binary as well as that of the visual companion can be easily recognized, whereas in the case of Mg II 4481 Å and He I 4471 Å only lines of the third body can be detected. The observed CCFs evidently indicate triple-lined profiles, as shown in Fig. 2. The central peak of the CCF appears to be the strongest and it does not show any RV variation. We thus attributed it to the visual component NSV 24512A, whose light was entirely collected by the optical fibre of the spectrograph, as a result of the very small separation.

We limited our analysis to the echelle orders in the spectral domains 5800–5950 and 4400–4520 Å, which include several photospheric absorption lines. We have disregarded very broad lines, such as Hβ and Hγ, because their broad wings affect the CCF and lead to large errors. As a first step, a three-component Gaussian fit was used to disentangle the CCF peaks. Inspection of the CCFs showed that the three components are visible and well separated from each other near the quadratures. A sample of three Gaussian fits is shown in Fig. 2. However, the CCFs are overlapped near the conjunction phases of the eclipsing pair. Therefore, a two-Gaussian fit for the primary and secondary components is wide and misplaced to the line centres because of the excess CCF strength between the components. We measured the RVs of the third component for all the spectra taken near the quadratures and we found a change of orbital motion to be taken into account over the duration of the spectra we obtained. By considering the effect of the third component on the CCF of the eclipsing pair's components, we decided to remove the third component from all the CCFs. Following the method proposed by Penny et al. (2001), we first made three-Gaussian fits of the well-separated CCFs using the deblending procedure in the IRAF routine SPLOT. The average fitted FWHMs are 120 ± 4, 70 ± 3 and 65 ± 1 km s^{-1} for the tertiary, primary and secondary components, respectively. As a second step, we took the average parameters for the third component at an RV of -19 ± 7 km s^{-1} and subtracted this constant Gaussian component from all the CCFs. After removal of the third component, all the CCFs were fitted with the

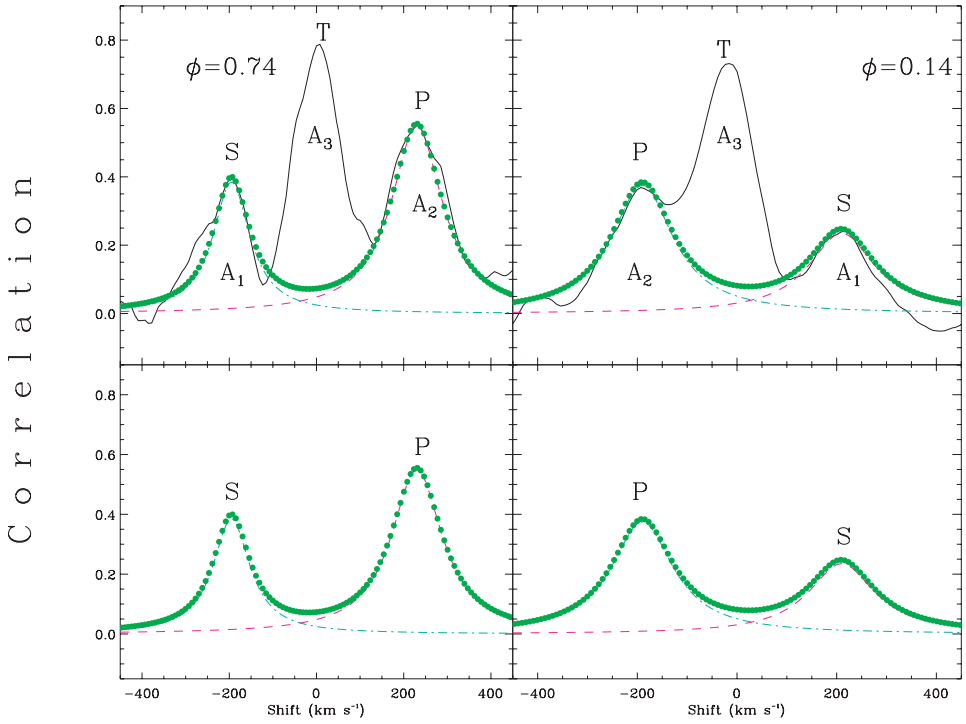

Figure 2. Example of 'deblending' a triple-peaked CCF between NSV 24512 and template spectrum α Lyr at $\phi = 0.74$ and $\phi = 0.14$ (showing a clear triple-lined profile in the top figures). P, S and T refer to primary, secondary and tertiary components, respectively. The fit to the observed spectrum for the primary and secondary components made up by two Lorentian functions is shown by dots. All RVs of the primary and secondary components have been measured by excluding the tertiary effect using this way. The deconvolved two Gaussian profiles of the primary and secondary components are displayed by dashed and dot-dashed line in the figure.

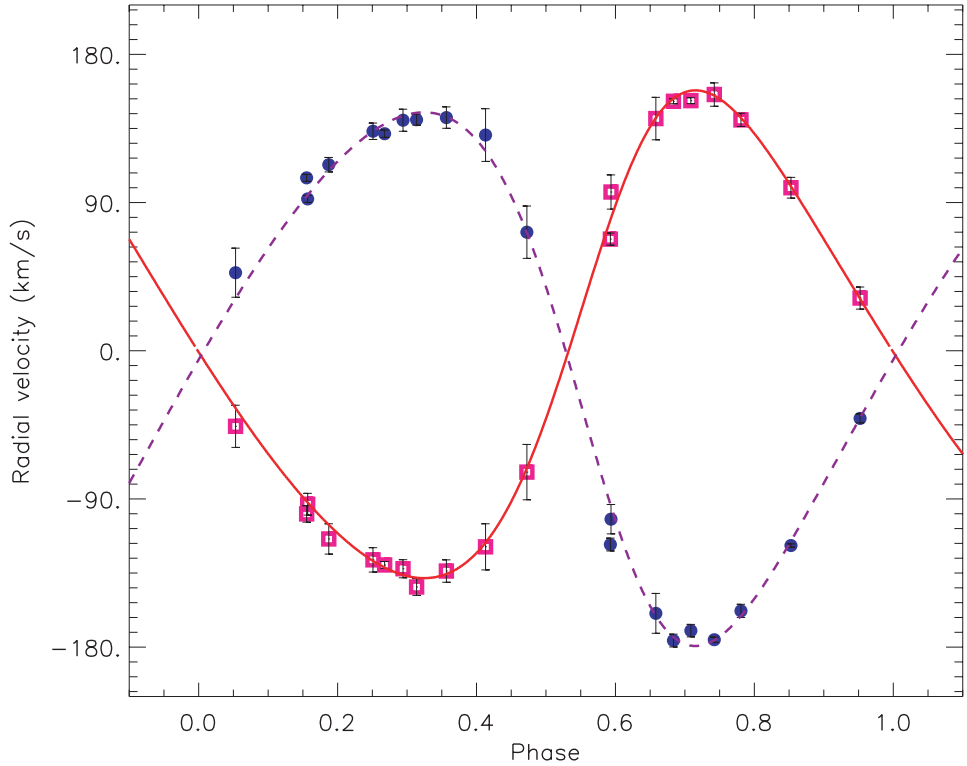

Figure 3. RV curves folded on a period of 2.2598 d, where phase zero is defined to be at primary mid-eclipse. The curves show the fit for a slightly eccentric orbit, to the primary (solid line) and secondary (dashed line) RVs. The dotted line indicates the systemic velocity. Symbols with error bars (error bars are masked by the symbol size in many cases) show the RV measurements for all three components of the system (primary, open squares; secondary, filled circles; tertiary, filled triangles).

double-Gaussian fitting procedure. Fig. 3 shows a sample of the double-Gaussian fit. Indeed, the shapes and velocities corresponding to the peaks of the CCFs are slightly changed. We estimated the intensity ratio $L_3/(L_1 + L_2) = 1.34$ from the three-Gaussian fits of the well-separated CCFs, and $L_2/L_1 = 0.78$ from the two-Gaussian fits of the CCFs after removal of a central Gaussian component. The heliocentric RVs for the primary (V_p) and the secondary (V_s) are listed in Table 1, along with the dates of observation and the corresponding orbital phases computed with the new ephemerides given in Section 3. The RVs of the components are the weighted averages of the values obtained from the cross-correlation of orders 6, 17 and 18 of the target spectra with the corresponding order of the standard star spectrum. The weight $W_i = 1/\sigma_i^2$ has been given to each measurement. The standard errors of the weighted means have been calculated on the basis of the errors (σ_i) in the RV values for each order according to the usual formula (e.g. Topping 1972). The σ_i values are computed by FXCOR according to the fitted peak height, as described by Tonry & Davis (1979). The observational points and their error bars are displayed in Fig. 3 as a function of orbital phase. We measure the semi-amplitudes of the primary (more massive) and secondary (less massive) components to be $K_1 = 148 \pm 3$ km s^{-1} and $K_2 = 163 \pm 4$ km s^{-1}, respectively.

The width of the cross-correlation profile is a good tool for the measurement of the projected rotational velocity $v \sin i$ (e.g. Queloz et al. 1998). The rotational velocities of the two components were obtained by measuring the FWHM of the CCF peaks in nine high-S/N spectra of NSV 24512 acquired close to the quadratures, when the spectral lines have the largest velocity separations. In order to construct a calibration curve of FWHM–$v \sin i$, we have used an

Table 1. Heliocentric RVs of NSV 24512. The columns give the heliocentric Julian date, the orbital phase (according to the ephemeris in equation 1), the radial velocities of the components with the corresponding errors and the average S/N of the spectrum.

HJD 240 0000+	Phase	Star 1		Star 2		⟨S/N⟩
		V_p	σ	V_s	σ	
53953.3506	0.3137	−143.5	5.1	140.3	3.3	79
53953.4475	0.3566	−133.8	6.8	141.6	6.5	100[a]
53954.3193	0.7423	155.6	7.1	−175.5	1.6	100[a]
53955.3247	0.1873	−114.3	9.2	113.0	4.4	106[a]
53955.4685	0.2509	−127.0	7.4	133.3	5.0	116[a]
53956.4462	0.6835	151.5	1.5	−176.0	3.9	86
53958.5028	0.5936	96.4	10.4	−102.3	8.9	106
53959.3131	0.9522	32.0	6.7	−41.1	2.7	110
53960.3544	0.4130	−119.1	14.0	131.0	16.0	121[a]
53963.4450	0.7807	140.2	4.0	−158.0	4.0	117
53970.3872	0.8527	99.0	6.3	−118.3	1.0	79
53971.3848	0.2942	−132.4	5.5	140.0	6.7	89
53973.3309	0.1554	−99.1	5.0	105.0	2.1	74
53974.4671	0.6582	141.0	12.9	−159.5	12.1	54
53980.3640	0.2677	−130.1	2.1	131.8	2.2	112[a]
53981.3604	0.7086	151.9	1.8	−170.0	3.8	97
53982.3734	0.1569	−93.2	6.6	92.2	2.1	100
53983.3582	0.5927	67.8	3.7	−117.7	3.9	113
53984.3986	0.0531	−45.9	12.8	47.4	14.9	88
53985.3463	0.4725	−73.7	16.8	72.0	15.9	97

[a]Used also for rotational velocity ($v \sin i$) measurements.

average spectrum of HD 27962 acquired with the same instrumentation. As the rotational velocity of HD 27962 is very low but not zero ($v \sin i \simeq 11$ km s^{-1}; Royer et al. 2004 and references therein), it could be considered as a useful template for A- and B-type stars rotating faster than $v \sin i \simeq 10$ km s^{-1}. The spectrum of HD 27962 was synthetically broadened by convolution with rotational profiles of increasing $v \sin i$ in steps of 5 km s^{-1} and the cross-correlation with the synthetically unbroadened one was performed at each step. The FWHM of the CCF peak was measured and the FWHM–$v \sin i$ calibration was established. The $v \sin i$ values of the two components of NSV 24512 were derived from the FWHM of their CCF peak and the aforementioned calibration relations for a few wavelength regions and for the best spectra. These resulted in 58 ± 5 km s^{-1} for the primary star and 46 ± 7 km s^{-1} for the secondary star.

3 PERIOD DETERMINATION AND APSIDAL MOTION

From our *BVR* observations, we obtained four times of primary mid-eclipse and four times of secondary mid-eclipse. These times of minimum, as a mean of three passbands, and their standard deviations are given in Table 2, together with those obtained by *Hipparcos* and ASAS-3 photometry, collected by Otero (2005). We determined the epoch and the orbital period of NSV 24512 by means of a weighted least-squares solution. The new ephemeris of the system was obtained as follows:

$$\text{Min } I \text{ (HJD)} = 245\,4298.3873(3) + 2.259772(3) \times E. \quad (1)$$

The orbital period found by us is slightly longer than that estimated by Otero (2005). The main difference is the epoch of the primary minimum. Our photometry clearly indicated that the depth of the primary eclipse is larger than that of the secondary eclipse. Therefore, the primary and secondary eclipses are interchanged with respect to the ephemeris given by Otero. The photometric observations and RV measurements of the system were folded with these light elements.

Otero (2005) noticed that there is a clear difference between the phases of the secondary minimum in the *Hipparcos* data and the ASAS-3 light curve, which were obtained roughly 10 years apart.

Table 2. Times of minima for NSV 24512.

HJD 240 0000+	Filter	σ	O − C	Type	Reference
48168.8080	H_p	0.0090	0.052	II	*Hipparcos*
49038.8220	H_p	0.0098	0.054	II	*Hipparcos*
51996.8520	*V*	–	.042	II	ASAS-3
52030.8110	*V*	–	0.105	II	ASAS-3
52701.9020	*V*	–	0.044	II	ASAS-3
52736.8700	*V*	–	−0.015	I	ASAS-3
52804.6940	*V*	–	0.016	I	ASAS-3
53092.8680	*V*	–	0.069	II	ASAS-3
53127.8110	*V*	–	−0.014	I	ASAS-3
53290.5210	*V*	–	−0.008	I	ASAS-3
53298.5220	*V*	–	0.084	II	ASAS-3
53492.8640	*V*	–	0.085	II	ASAS-3
54236.3542	*BVR*	0.0004	0.111	II	This study
54237.3898	*BVR*	0.0005	0.016	I	This study
54245.3728	*BVR*	0.0002	0.090	II	This study
54263.4532	*BVR*	0.0003	0.094	II	This study
54280.2955	*BVR*	0.0004	−0.014	I	This study
54298.3873	*BVR*	0.0004	−0.051	I	This study
54315.4110	*BVR*	0.0001	0.075	II	This study
54332.2741	*BVR*	0.0001	−0.010	I	This study

This difference indicates that NSV 24512 is most likely exhibiting fast apsidal motion, so we have tried to measure its apsidal period from the times of minimum light in Table 2. We used the APSMOT code (Southworth, Maxted & Smalley 2004) and included the orbital eccentricity measured from the RVs (see below). We have unfortunately not been able to obtain a useful result, because the times of minimum light only cover a small part of one apsidal period.

Further monitoring of times of eclipse, particularly for secondary minima, will be needed to measure the apsidal period. Alternatively, the relatively large orbital eccentricity means that apsidal motion may be detectable in spectroscopic RV measurements from data sets taken a few decades apart. Theoretical predictions of the apsidal motion rate are not available for massive pre-main-sequence stars, such as the components of NSV 24512, but for main-sequence stars of a similar mass we would expect an apsidal period of the order of a century. This apsidal motion rate is sufficiently small that the linear ephemeris (equation 1) can be used to analyse the photometry and spectroscopy presented in this work.

4 SIMULTANEOUS ANALYSIS OF LIGHT CURVE AND RADIAL VELOCITIES

The Tycho instrument of *Hipparcos* observed the components of visual double stars with separations above 0.3 arcsec (Fabricius et al. 2002). Because the separation between the components of NSV 24512 was below this limit, the Tycho instrument cannot make individual measurements of the components. Therefore, we have only H_p measurements of both components made by *Hipparcos*, which are inadequate for their spectral classification. The common spectral type of ADS 11410 AB is given as B5 V by Pavlova & Rspaev (1986) and B3 V by Lara et al. (1991). The first estimate of the spectral types of A and B have been made by Straizys et al. (1996) from Vilnius seven-colour photometry. They estimate the spectral types of the visual double pair as B3 V + B3 V and the difference between their apparent visual magnitudes as 0.0 mag. However, this difference was measured by *Hipparcos* as 0.125 mag, showing the components are very similar. However, the infrared colours of NSV 24512 given in the Two-Micron All-Sky Survey (2MASS) catalogue (Skrutskie 1999) appear to be similar to heavily reddened O-type stars.

From the calibration relationships between the equivalent widths of absorption lines and spectral type given by Hernández et al. (2004), we derived an 'average' spectral type of about B2-5 for the system of the three stars seen as a whole. Furthermore, we have compared the spectra of NSV 24512 taken near the conjunctions with spectral-type standard stars obtaining a similar result (see Fig. 4). This classification is in good agreement with the earlier classifications made by wide- and intermediate-band photometric studies. The resolution of our spectra was inadequate to obtain the spectra of components A and B separately. Thus, we could not attempt to perform a spectral classification of the visual pair's components. Therefore, from the analysis of the light curve we can only derive the difference of temperature between the two components of the inner binary. Their absolute values can be inferred from the 'average' spectral type and the variation of the colour indices with a very large uncertainty (more than 1500–2000 K). From the good RV curves, we can instead derive very good values for the masses of the system's components.

As the spectroscopic observations indicate that component B is the eclipsing binary, we first subtracted the light contribution of component A from the total light. In the *V* passband, the light

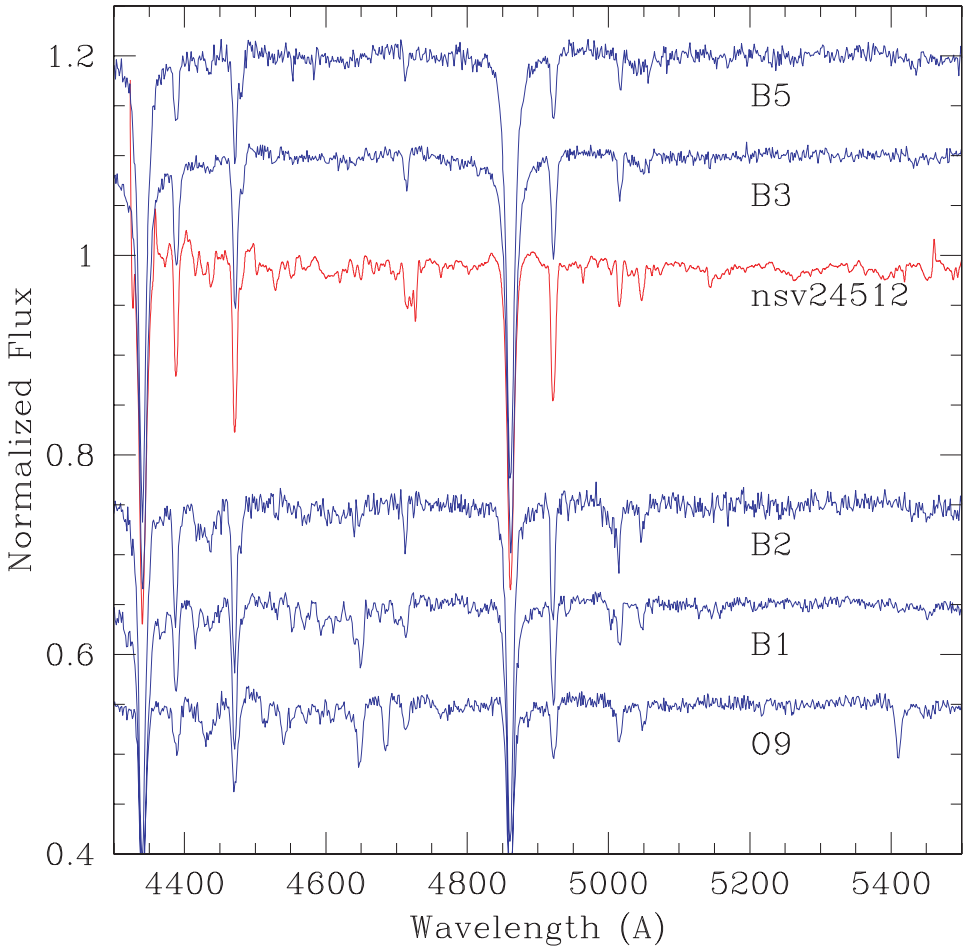

Figure 4. Spectral classification of the system.

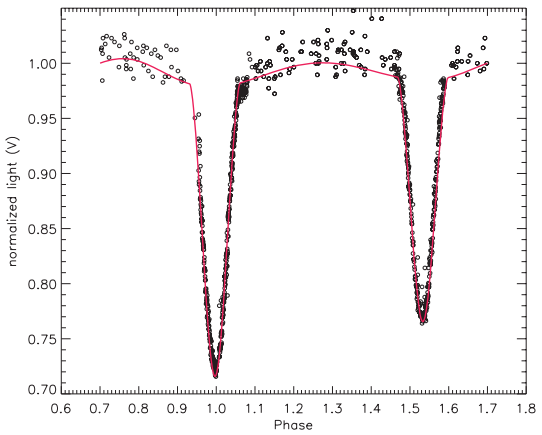

Figure 5. The reduced *V* passband light curve compared with the computed curve.

contribution of component A is about 0.529. The reduced *V* passband light curve is shown in Fig. 5. The effective temperatures of the primary and secondary components of the eclipsing pair were derived from the calibrations of Drilling & Landolt (2000) using preliminary estimates of their masses. The primary component of the eclipsing pair seems to have a mass of about 3.6 $M_{\odot}$, which corresponds to a spectral type of about B8, while the secondary component has a mass of about 3.3 $M_{\odot}$, corresponding to a B9-type star.

We chose the Wilson–Devinney code implemented into the PHOEBE package by Prsa & Zwitter (2005) to model the light and RV curves. The modified version of this program allows us to calculate RV curves and monochromatic light curves of stars simultaneously, either for a circular or an eccentric orbit, in a graphical environment. In this model, the code was set in Mode-2 for detached binaries with no constraints on their surface potentials. The simplest considerations were applied for the parameters of the stars in the model: the stars were considered to be black bodies and the approximate reflection model (MREF = 1) was adopted. Gravity-darkening exponents $g_1 = g_2 = 1$ and bolometric albedos $Alb_1 = Alb_2 = 1$ were assumed as typical for early-type stars with radiative envelopes. We used the square-root limb-darkening law because the stars are hotter than 8500 K (see Van Hamme 1993). Bolometric and *V*-band limb-darkening coefficients were taken from Van Hamme (1993). A mass ratio of $q = 0.914$ and an eccentricity of $e = 0.193$, determined from preliminary analyses, were taken as initial values. The rotation of both components was assumed to be synchronous with the orbit: $F_1 = F_2 = 1$.

Assuming the components are in the region between the zero-age main sequence and the terminal-age main sequence, we assign a range of effective temperatures between 9800 and 12 200 K for the more massive component. We started the analysis of the *V*-band light curve and RVs simultaneously with an effective temperature

Table 3. Parameters of NSV 24512.

Parameter	Analysis
P (d)	2.259772[a]
e	0.193 ± 0.002
a ($R_\odot$)	13.89 ± 0.01
w	297 ± 2
γ (km s^{-1})	-3.02 ± 0.19
K_1 (km s^{-1})	$\mathbf{148 \pm 3}$
K_2 (km s^{-1})	$\mathbf{163 \pm 4}$
$\Delta\,\phi$	0.0149 ± 0.0001
i (deg)	79.9 ± 1.1
Ω_1	5.3752 ± 0.0019
Ω_2	5.6396 ± 0.0021
$q = M_2/M_1$	0.9141 ± 0.0084
$\langle r_1 \rangle$	0.2310 ± 0.0002
$\langle r_2 \rangle$	0.2110 ± 0.0003
T_1 (K)	11 100 (fixed)
T_2 (K)	$10\,350 \pm 155$
$L_1/(L_1 + L_2)$	0.553 ± 0.004

[a]Fixed at the value found in Section 3.

of 9800 K, and then increased it in steps of 200 K. The adjustable parameters in fitting the light and RV curves were the surface potentials (Ω_1 and Ω_2), the effective temperature of the secondary (T_2), the luminosity of the primary (L_1), orbital inclination (i), the eccentricity (e), the mass ratio (q), the longitude of periastron (ω), the zero epoch offset ($\Delta\,\phi$), the semimajor axis of the orbit (a) and the systemic velocity (V_γ). The iterations were carried out automatically until convergence, and a solution was defined as the set of parameters for which the differential corrections were smaller than the probable errors. The best fit was achieved at an effective temperature of 11 100 K for the more massive component, which corresponds to a B8 star. The final orbital and stellar parameters from the simultaneous V light and RV curve analysis are listed in Table 3. The parameters that were adjusted have standard errors provided by the code. The computed best-fitting model light and RV curves corresponding to the simultaneous light-velocity solution are compared with the observations in Figs 3 and 5.

5 DISCUSSION AND CONCLUSIONS

We derived the astrophysical parameters and radiative properties of the components of the recently discovered eclipsing binary NSV 24512 from a simultaneous analysis of the light and RV curves, which provided us with the values reported in Table 3. The astrophysical parameters of the components are listed in Table 4. The luminosities and absolute bolometric magnitudes were calculated directly from the radii and effective temperatures of the components. The standard deviations on the effective temperatures of the components were estimated from the errors on the masses of the components. The uncertainties in the parameters in this table were evaluated by using the JKTABSDIM[2] code, which calculates distances and other physical parameters using several different sources of bolometric corrections (Southworth, Maxted & Smalley 2005).

The light ratio of $L_2/L_1 = 0.81$ obtained from the V-band light-curve analysis is in good agreement with that estimated from the FWHM as 0.78. However, we find the light ratio of the visual components as 1.22 from the apparent magnitudes given by Hartkopf et al. (2005) and 1.12 from those measured by *Hipparcos*. The former is very close to that obtained by us using the FWHMs.

As the system is located in a young molecular cloud and is a well-detached eclipsing binary, it is reasonable to assume that the evolutionary status of the components can be estimated from evolutionary models of single stars without accounting for any interaction or mass transfer. Fig. 6 shows two isochrones with different ages and the evolutionary tracks for single stars of masses 4 and 3 $M_\odot$, taken from the models of Siess et al. (2000) for $Z = 0.03$. The absolute parameters of the components place the stars very close to the pre-main-sequence evolutionary tracks of 3.6 and 3.3 $M_\odot$ single stars, in very good agreement with the dynamically determined masses. The set of tracks for high metal abundance gives a better reproduction of the data. The evolutionary tracks indicate that the components have an age of about 2.1 Myr, in good agreement with

Table 4. Astrophysical data for NSV 24512. The errors of the luminosities are dominated by the errors on the temperatures. Quantities were calculated assuming $L_\odot = 3.826 \times 10^{26}$ W and $M_{bol\odot} = 4.75$.

	NSV 24512	
Parameter	Primary	Secondary
Mass ($M_\odot$)	3.68 ± 0.05	3.36 ± 0.04
Radius ($R_\odot$)	3.21 ± 0.05	2.93 ± 0.05
Luminosity ($L_\odot$)	141 ± 7	89 ± 7
Temperature (K)	$11\,100 \pm 300$	$10\,350 \pm 280$
$\log g$ (cgs)	3.9914 ± 0.0028	4.0310 ± 0.0031
V_0 (mag)	7.08 ± 0.03	7.31 ± 0.03
$(B-V)_0$ (mag)	-0.09 ± 0.03	-0.05 ± 0.03
$(U-B)_0$ (mag)	-0.28 ± 0.03	-0.13 ± 0.03
M_{bol} (mag)	-0.61 ± 0.04	-0.11 ± 0.04
BC	-0.707	-0.474
M_V (mag)	0.10 ± 0.04	0.36 ± 0.04
Distance (pc)	247 ± 5	

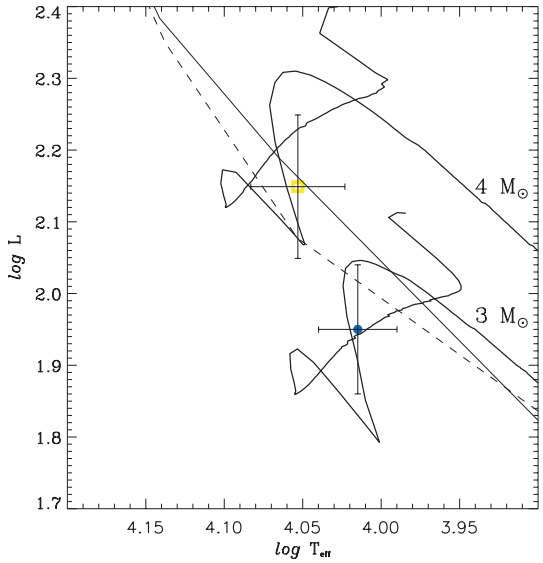

Figure 6. Theoretical evolutionary tracks with $Z = 0.03$ for the system (labelled in units of solar mass for 4 and 3 $M_\odot$) and isochrones from Siess et al. (2000). The square and filled circle denote the primary and secondary components of NSV 24512. The best fit occurs at an age of 2.1×10^6 (continuous line) to 2.4×10^6 (dashed line) for the system. The error bars of the measured quantities are shown by vertical and horizontal lines.

[2] See http://www.astro.keele.ac.uk/∼jkt/codes.html.

the very young age of the Serpens cloud, which is known to be one of the most active star-forming regions in the solar vicinity. The northern part of the Serpens group is occupied by a molecular cloud, which contains some far- and near-infrared sources, several small reflection and emission nebulae, and Herbig–Haro objects. Some Hα emission stars and Herbig Ae-type stars were also detected in the molecular cloud.

The projected rotational velocities of the primary and secondary components were measured to be 44 ± 5 km s^{-1} and 38 ± 7 km s^{-1}, respectively. Using the radii of the components, we computed a synchronous rotation velocity of 70 km s^{-1} for the primary component and 64 km s^{-1} for the secondary component. The observed rotational velocities are very small when compared with those computed. It is clear, therefore, that the components of NSV 24512 are far from synchronous rotation. The slow rotation rates of the components may also be taken as evidence that the system is composed of pre-main-sequence stars.

We used an interstellar colour excess of $E(B–V) = 0.79$ and an interstellar extinction of $A_V = 2.46$ mag (Straizys et al. 1996) to deredden the apparent visual magnitudes and colour indices of the components given in Table 4. The astrophysical parameters and the radiative properties indicate that the eclipsing binary consists of very similar components with B8 and B9 spectral types. Using the total apparent visual magnitude of the system measured by *Hipparcos* (8.893 ± 0.033 mag), the light ratio and interstellar extinction, we derive the distance to the system as 247 ± 5 pc. The parallax of NSV 24512 from the *Hipparcos* satellite is very uncertain: $\pi_{\rm Hip} = 6.3 \pm 10.1$ mas. The distance to the Serpens cloud was measured by various investigators, using different methods, to be 440 pc (Racine 1968), 440 pc (Strom, Grasdalen & Strom 1974), 425 pc (Chavarria et al. 1988), 700 pc (Zhang et al. 1988), 313 pc (Lara et al. 1991) and 259 ± 37 pc (Straizys et al. 1996). In the last of these investigations, Straizys et al. assumed that the spectral type of the components is B3 V and that they have the same apparent visual magnitudes. This leads to a distance of 279 pc, which agrees with the value found by us within 1σ. The distance to the system derived by us is very close to that obtained by Chavarria et al. (1988) as 245 ± 30 pc, using photometric and spectroscopic data. It should be noted that Chavarria et al. (1988) assumed that the system was a single star.

ACKNOWLEDGMENTS

We thank Professor G. Strazzulla, director of the OAC, and Dr G. Leto, responsible for the M. G. Fracastoro observing station, for their warm hospitality and for allowing us telescope time for the observations. In addition, ÖÇ is grateful to all the people working at the OAC for creating a stimulating and enjoyable atmosphere. In particular, ÖÇ is grateful to the technical staff of the OAC, namely P. Bruno, G. Carbonaro, A. Distefano, M. Miraglia, A. Miccichè and G. Occhipinti, for valuable support in carrying out the observations. The authors also acknowledge generous allotments of observing time at Ege University Observatory. This research has also been partially supported by INAF and Italian MIUR. JS acknowledges financial support from STFC. This research has made use of the ADS and CDS data bases, operated at the Centre de Données Astronomiques, Strasbourg, France. This paper is dedicated to the memory of Dr Z. Müyesseroğlu who passed away last year. We are grateful to him for his encouraging support and his contributions to observational astronomy in Turkey.

REFERENCES

Andersen J., 1975, A&A, 44, 355
Chavarria K. C., de Lara E., Finkenzeller U., Mendoza E. E., Ocegueda J., 1988, A&A, 197, 151
de Jager C., Nieuwenhuijzen H., 1987, A&A, 177, 217
Drilling J. S., Landolt A. U., 2000, in Cox A. N., ed., Allen's Astrophysical Quantities, 4th edn. Springer, Berlin, p. 388
Fabricius C., Hog E., Makarov V. V., Mason B. D., Wycoff G. L., S. E. Urban, 2002, A&A, 384, 180
Hartkopf W. I., Mason B. D., McAlister H. A., 2005, AJ, 111, 370
Hernández J., Calvet N., Briceño C., Hartmann L., Berlind P., 2004, AJ, 127, 1682
Knude J., 1992, A&AS, 92, 841
Lara E., Chavarria K. C., Lopez-Molina G., 1991, A&A, 243, 139
Massey P., Davis L. E., 1992, A User's Guide to Stellar CCD Photometry with IRAF. Available online at http://iraf.noao.edu/iraf/ftp/iraf/docs/daophot2.ps.Z.
Otero S. A., 2005, Inf. Bull. Var. Stars, 5631
Pavlova L. A., Rspaev F. K., 1986, Astrofizika, 25, 461
Penny R. L., Seyle D., Gies D. R., Harvin J. A., Bagnuolo W. G. Jr, Thaller M. L., Fullerton A. W., Kaper L., 2001, ApJ, 548, 889
Perryman M. A. C. et al., 1997, A&A, 323, L49
Pojmanski G., 2002, AcA, 52, 397
Popper D. M., Jeong Y.-C., 1994, PASP, 106, 189
Prsa A., Zwitter T., 2005, ApJ 628, 426
Queloz D., Allain S., Mermilliod J.-C., Bouvier J., Mayor M., 1998, A&A, 335, 183
Racine R., 1968, AJ, 73, 233
Royer F., Grenier S., Baylac M., Gomez A. E., Zorec J., 2004, A&A, 393, 897
Rufener F., Bartholdi P., 1982, A&AS, 48, 503
Siess L., Dufour E., Forestini M., 2000, A&A, 358, 593
Skrutskie M. F., 1999, A&AS, 195, 340
Southworth J., Maxted P. F. L., Smalley B., 2004, MNRAS, 351, 1277
Southworth J., Maxted P. F. L., Smalley B., 2005, A&A, 429, 645
Straizys V., Cernis K., Bartasiute S., 1996, Baltic Astron., 5, 125
Strom S. E., Grasdalen G. L., Strom K. M., 1974, ApJ, 191, 11
Tokovinin A. A., 1997, A&AS, 124, 75
Tonry J., Davis M., 1979, AJ, 84, 1511
Topping J., 1972, Errors of Observation and Their Treatment. Chapman & Hall, London, p. 89
Van Buren D., McCray R., 1988, ApJ, 329, L93
Van Buren D., Noriega-Crespo A., Dgani R., 1995, AJ, 110, 2914
Van Hamme W., 1993, AJ, 106, 2096
Zhang C. Y., Laureijs R. J., Clark F. O., Wesselius P. R., 1988, A&A, 199, 170

This paper has been typeset from a TEX/LATEX file prepared by the author.